

Episodic Melt Transport at Mid-Ocean Ridges Inferred from Magnetotelluric Sounding

Graham Heinson

Department of Geology and Geophysics, University of Adelaide, Adelaide, Australia

Steven Constable

Scripps Institution of Oceanography, UCSD, La Jolla CA, USA

Antony White

School of Chemistry, Physics and Earth Sciences, Flinders University of South Australia, Adelaide, Australia

Abstract. Oceanic crust is generated at mid-ocean ridges by decompression melting of upwelling mantle at depths of between 50 and 120 km. Geodynamic and geochemical models of upwelling, melt extraction, and melt emplacement into crustal magma reservoirs present a variety of possible migration geometries, most of which assume steady-state or near steady-state processes. Here we present results from marine magnetotelluric (MT) measurements, carried out as part of the RAMESSES experiment on the slow spreading Reykjanes Ridge, which support a model of melt extraction and migration that is episodic, rather than steady-state.

Introduction

In 1993 a multidisciplinary geophysical survey was conducted on the northern section of the mid-Atlantic ridge, known as the Reykjanes Ridge, centered on an axial volcanic ridge (AVR) at 57° 45'N. The RAMESSES (Reykjanes Axial Melt Experiment: Structural Synthesis from Electromagnetics and Seismics) focused on a ridge segment that had been identified from the previous cruise leg as being tectonically active from dredged samples of fresh, glassy seafloor basalts and bright side-scan reflections. This segment is about 40 km long, 4 - 5 km wide, and a few hundred metres high, offset from other ridges to the north and south which are in en echelon arrangement.

Seismic and controlled source electromagnetic (CSEM) data and results (Navin et al., 1998; MacGregor et al., 1998) and a geodynamic synthesis (Sinha et al., 1997, 1998) have been reported elsewhere. For the MT component of the study, we recovered data from 2 full-component MT instruments on the ridge axis, one at the centre of the geophysical array/volcanic segment and one 10 km to the south. Data from an off-axis magnetometer and four off-axis CSEM electrometers also provided constraints on the spatial variations of magnetic and electric fields across the AVR. Figure 1 shows the location of the experiment, instrument positions and water depths.

Data

The MT method requires the simultaneous time-series measurement of horizontal components of magnetic (B) and electric (E) variational fields that result from naturally-occurring EM signals in the ionosphere. Typical seafloor MT measurements are limited to a frequency bandwidth of 10^{-1} - 10^{-5} Hz (10 - 10^5 s), providing maximum sensitivity between about 1 and 400 km into the Earth. The ratio of orthogonal components of E and B in the frequency domain is a measure of Earth's electrical resistivity at that site. With pairs of orthogonal E and B fields, MT responses may be obtained in two polarisations, or modes. Above 1D layered structures the two MT modes are identical, but for 2D structures the MT fields may be rotated to modes of electric field parallel to strike (TE mode) and perpendicular to strike (TM mode).

Figure 2 shows MT apparent resistivities and phases from site Roderick (above the centre of the AVR). Twenty-one days of data, sampled every 10 s, were processed with robust

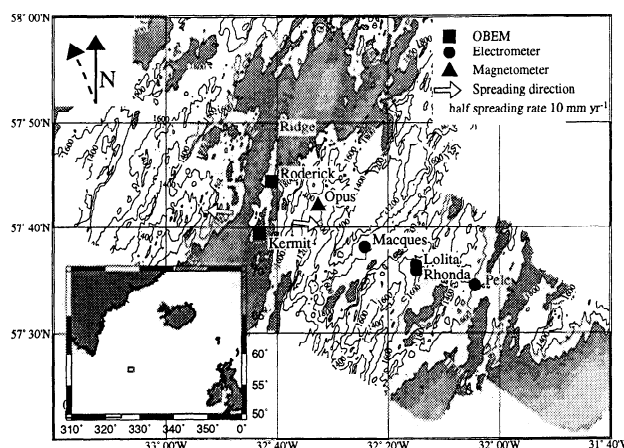


Figure 1. Location of ocean bottom MT instruments (OBEM), magnetometers and electrometers. Topographic contours are shown every 200 m, and depths greater than 1800 m are shaded. Spreading orientation is shown by the white arrows, and the direction of geomagnetic north by the black dashed arrow. The inset map shows the location of the survey relative to the coastlines of Greenland and Europe in Mercator projection.

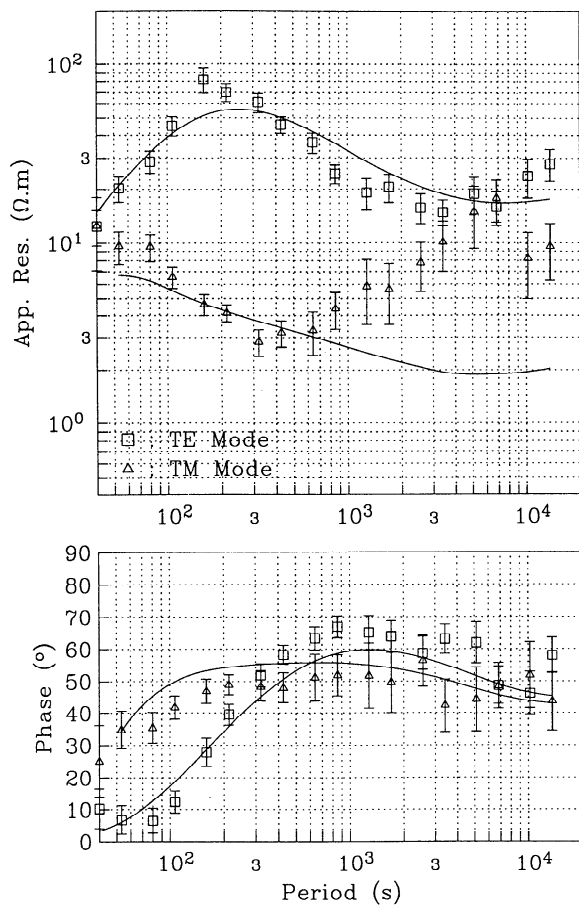


Figure 2. MT response estimates from Roderick with one standard error bar. The TE data (squares) represent responses along the strike of the ridge, the TM data (triangles) are in the orthogonal orientation. Solid lines represent the 2D forward model (Figure 5) fits to both TE and TM modes.

remote-reference schemes (Chave and Thomson, 1989; Egbert and Booker, 1986), and examined for galvanic distortion (Groom and Bailey, 1989; Lilley, 1998; Chave and Smith, 1994). Distortion analyses show 2D induction at all sites with negligible shear and twist, and a strike direction of 55° parallel to the ridge axis and approximately parallel to the distant coastlines of Greenland and Europe. Thus, MT data are dominantly 2D with the 'TE mode' associated with ridge-parallel electric fields and the 'TM mode' ridge-perpendicular electric fields.

There appears to be little electric or magnetic galvanic distortion. MT transfer functions between magnetic field data at site Roderick, remote-reference magnetic field data from Opus, and TE mode electric fields at sites Pele, Rhonda, Maques, Roderick and Kermit show a remarkably uniform electric field (Figure 3). A similar comparison for TM electric fields at sites Lolita, Roderick and Kermit in Figure 3 show an order of magnitude resistivity variation (static shift), probably due to electric charge build-up along scarps of normal-faulted grabens bounding the AVR.

Inversion

Data in Figure 2 are clearly influenced by non-uniform induction effects, but the TE mode (with electric field parallel

to the ridge-axis) is least affected by coast-effect from Greenland and Europe and local topography. We argue that the presence of Iceland to the north is less important due to its small coastal extent compared to Greenland, and very low crustal resistivity due to the hotspot (Beblo et al., 1983). The TE mode data were inverted using the 1D Occam's inversion (Constable et al., 1987), with rms misfits of 1.3 for Roderick and 1.9 for Kermit. Inversions are shown in Figure 4, along with comparison models obtained above Axial Seamount on the Juan de Fuca Ridge (Heinson et al., 1996; Constable et al., 1997), and for a site on 'normal' oceanic lithosphere in the centre of the Pacific Plate, about 800 km southwest of Hawaii.

The RAMASSES models are in close agreement below 30 km, with a minimum ($< 10 \Omega.m$) at about 60 km depth. Thus, for this section of the AVR the mantle is not significantly heterogeneous in temperature or melt-porosity on horizontal-scales of 10 km. In both models there is a slight increase in resistivity below 100 km to about $15 \Omega.m$. Above 30 km, the site Roderick has low resistivity close to the surface, whereas at Kermit much higher resistivities are evident.

Axial Seamount and Pacific Plate inversions provide two end-member models for comparison. Axial Seamount MT data (collected in 1994) are very uniform, indicative of low resistivity ($10 - 20 \Omega.m$) from seafloor to mid-mantle, but the lowest resistivities ($< 10 \Omega.m$) are present at the same depth as for the RAMASSES sites. It was suggested (Heinson et al., 1996) that such low resistivities were due to connected melt through the mantle beneath Axial Seamount, which is consistent with evidence of fresh lava flows in 1998 (Embley et al., 1999) showing that Axial Seamount is currently active. In contrast, Pacific Plate MT data are much more resistive over the top 100 km, but similar (about $20 \Omega.m$) below 200 km. High resistivities in the uppermost mantle suggest lower temperatures and a lack of molten asthenosphere.

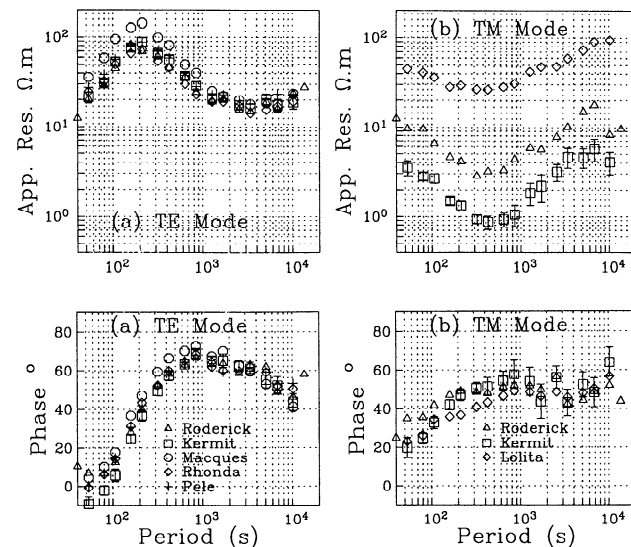


Figure 3. (a) MT transfer function between the TE mode electric fields (parallel to the AVR axis) at sites Pele, Rhonda, Maques, Roderick and Kermit and the orthogonal component of magnetic field at site Roderick; (b) MT transfer function between the TM mode electric fields (perpendicular to the AVR axis) at sites Lolita, Roderick and Kermit and the orthogonal component of magnetic field at site Roderick.

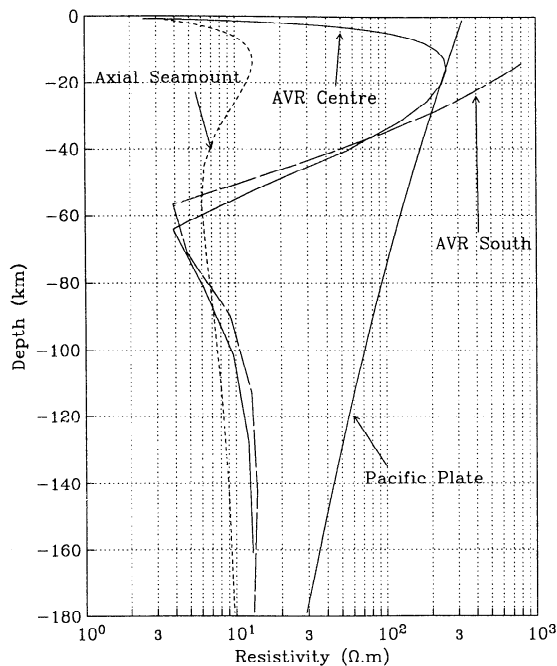


Figure 4. Occam's 1D inversions for the RAMASSES sites Roderick (AVR centre) and Kermit (AVR South). Also shown are inversions for Axial Seamount, Juan de Fuca Ridge (indicative of connected melt from the asthenosphere at 60 km to the crust), and for normal oceanic lithosphere in the centre of the Pacific Plate (showing an absence of an electrical asthenosphere, and a highly resistive lithosphere).

Forward Modelling

One of the perennial problems of marine MT is the difficulty in simultaneously modelling local structure of dimension 0.1 - 1 km and the effect of the conductive global ocean on horizontal scales of 1000 km (Heinson and Constable, 1992). In this case, however, we have independent constraints on local structure from the CSEM sounding (MacGregor et al., 1998) and seismics (Navin et al., 1998). Both model sections across the central segment of the AVR to the Moho image a melt lens and crystalline mush zone at a depth of 2.5 km beneath the AVR. The melt lens (100 m thick and 4 km wide) and mush zone (3 km thick and approximately 8 km wide at the top, tapering with depth) appears to extend at least 11 km along the ridge axis. Seismic peg-leg multiples (Navin et al., 1998) indicate that some melt is present beneath the entire AVR segment of 20 km, but it is less clear whether the magma chamber reduces in size away from the centre of the ridge segment.

If we take the 2D resistivity model independently determined from CSEM sounding we need only add a low resistivity (5 - 20 $\Omega.m$) asthenosphere at a depth of 40 km (Figure 5) and the TE mode data at site Roderick are fit (using a 2D finite element code, Wannamaker et al., 1986) within the error bounds (Figure 2). The CSEM model with a low resistivity crystalline mush zone does not fit observed data from Kermit. Seismic evidence suggests the presence of a melt lens beneath Kermit, but is less sensitive to a bigger residual mush zone. If the mush zone resistivities of 2.5 $\Omega.m$ are replaced by 200 $\Omega.m$ in Figure 5, but maintaining the melt lens of 1 $\Omega.m$, then a reasonable fit to the Kermit TE mode data is achieved.

Fitting TM mode data is more complicated due to coast-effect, ridge topography and crustal heterogeneity. We note that the CSEM resistivity model alone does not reproduce low apparent resistivities of 0.1 - 10 $\Omega.m$ observed in the TM modes. Instead, the uniformity of the TM mode electric fields (other than static-shift) indicates that the TM mode is largely influenced by regional-scale coast-effect induction coupled with a resistive oceanic lithosphere.

Including the Greenland coastline in Figure 5 fits the TM mode data with a 40 km thick lithosphere of resistivity 10,000 $\Omega.m$, constrained within a factor of about five. Increasing the resistivity to 50,000 $\Omega.m$ reduces the modelled TM mode apparent resistivities to less than 1 $\Omega.m$, too small even allowing for static-shift. Similarly, a resistivity lower than 5,000 $\Omega.m$ reduces coast-effect and hence anisotropy between TE and TM modes. The resistivity-thickness of the model lithosphere is $3 \times 10^8 \Omega.m^2$, consistent with, but slightly smaller than, previous determinations (Cox et al., 1986).

Finally, 2D forward models indicate that a low resistivity magma chamber is required beneath Roderick but not Kermit. As the magma chamber has limited along-axis extent, we used a 3D forward model (Mackie et al., 1993) to investigate the effect on the TE mode. The CSEM section in Figure 5 was expanded as a 3D model, with the magma chamber of length 11 km, centred about the AVR. We find that as skin-depths at the shortest periods are less than the width and thickness of the magma chamber, TE responses above the centre of the magma chamber are largely unaffected by its along-axis extent. A few kilometres from the end of the magma chamber, the TE mode is dominated by the resistive crustal structure.

Discussion and Conclusions

As the MT method is sensitive to electrical conductance, it directly senses the total volume of connected melt in the magma chamber, independent of geometry. Our MT data

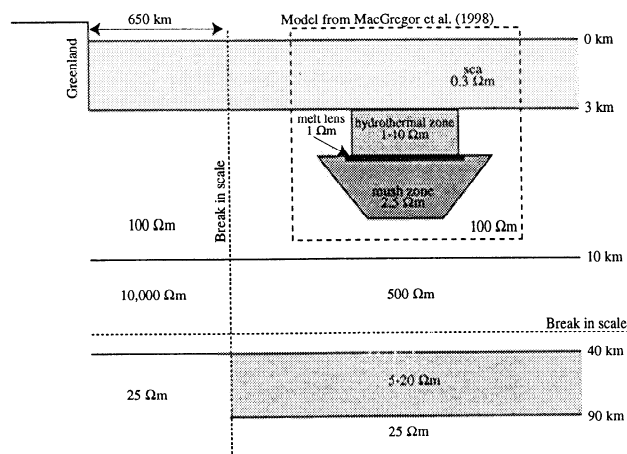


Figure 5. The 2D-resistivity structure used in forward modelling. Structural boundaries and resistivities in the crust are imposed from seismic and CSEM constraints. Below the Moho, the resistivity structure is based directly on the 1D inversions in Figure 4. For site Kermit, the magma chamber was omitted in the forward model. Data fits to MT TE and TM mode responses are shown in Figure 2.

therefore provides verification that crustal melt calculations of MacGregor et al. (1998) are robust, and that there is indeed 20,000 years worth of material for crustal accretion presently available in the crust. As such a magma body would freeze over about 1500 years, this is clear evidence of cyclicity or episodicity in melt transport between mantle and crust. MT results preclude a significant fraction of connected melt in the uppermost mantle beneath the ridge, and so supports episodic, rather than merely cyclic, magma emplacement. Given the highly non-linear relationship between permeability and the diameter of any pores or conduits, it seems likely that the efficiency of magma transport and emplacement far exceeds the steady-state demand for new crustal material, even at fast ridges. One can instead envisage melt build-up in distributed pores in the mantle reaching a critical level of gravitational instability and then coalescing into a few efficient diapirs for emplacement into the crust.

The results from the RAMASSES experiment can be placed in context with other marine MT interpretations. The Pacific Plate resistivity profile is perhaps characteristic of lithosphere at sub-solidus temperatures. A lack of adiabatic/decompression/upwelling derived melting leads to uppermost mantle resistivities at least one order of magnitude higher than observed beneath mid-ocean ridges. Above 80 km, the three mid-ocean ridge profiles in Figure 4 show a consistent picture of the presence of partial melt and higher temperatures. Below Axial Seamount, there is effectively no resistive lithosphere: a substantial and connected melt fraction is present in the mantle right up to the base of the crust. By comparison, beneath the RAMESSES sites marginally lower resistivity indicates that there is, if anything, more melt in the mantle at around 60 km depth. Above this is a 40 km thick resistive lithosphere with effectively no melt in it that separates the mantle-melting zone from the crustal magma chamber. This would be expected if the upper few tens of kilometres of the mantle at the Reykjanes Ridge were periodically drained of magma, which is extracted upwards rapidly to create large but ephemeral crustal magma chambers, and to drive tectono-magmatic cycles with periods of tens of thousands of years.

Acknowledgments. We would like to thank the officers and crew of the R/V Charles Darwin, the seagoing technical staff of the Research Vessel Services and other members of the Scientific Party of cruise CD81/93. G. Heinson and A. White were funded by the Australian Research Council, and S. Constable received funding from the National Science Foundation under grant number OCE91-02551. At Flinders University, Brenton Perkins and Bob Walker, and at Scripps Institution Jacques Lemire and Tom Deaton are thanked for equipment electronics and hardware design and construction.

References

- Beblo, M., A. Bjornsson, K. Arnason, B. Stein and P. Wolfgram, Electrical conductivity beneath Iceland - constraints imposed by magnetotelluric results on temperature, partial melting, crustal and mantle structure, *J. Geophys. Res.*, 53, 16-23, 1983.
- Chave, A.D. and J.T. Smith, On electric and magnetic galvanic distortion tensor decompositions, *J. Geophys. Res.*, 99, 4,669-4,682, 1994.
- Chave, A.D. and D.J. Thomson, Some comments on magnetotelluric response function estimation, *J. Geophys. Res.*, 94, 14,215-14,225, 1989.
- Constable, S.C., R.L. Parker and C.G. Constable, Occam's Inversion: a practical algorithm for generating smooth models from EM sounding data, *Geophysics*, 52, 289-300, 1987.
- Constable, S.C., G.S. Heinson, G. Anderson and A. White, Seafloor electromagnetic measurements above Axial Seamount, Juan de Fuca Ridge, *J. Geomag. Geoelectr.*, 49, 1327-1342, 1997.
- Cox, C.S., S.C. Constable, A.D. Chave and S.C. Webb, Controlled-source electromagnetic sounding of the oceanic lithosphere, *Nature*, 320, 52-54, 1986.
- Egbert, G.D. and J.R. Booker, Robust estimation of geomagnetic transfer functions, *Geophys. J. R. Astron. Soc.*, 87, 173-194, 1986.
- Embley, R.W., Chadwick, W.W., Jr., Clague, D. and Stakes, D., 1998 Eruption of Axial Volcano: Multibeam anomalies and seafloor observations, *Geophys. Res. Lett.*, 26, 3425-3428, 1999.
- Groom, R.W. and R.C. Bailey, Decomposition of magnetotelluric impedance tensors in the presence of local three-dimensional galvanic distortion, *J. Geophys. Res.*, 94, 1,193-1,925, 1989.
- Heinson, G.S., S.C. Constable and A. White, Seafloor magnetotelluric sounding above Axial Seamount, *Geophys. Res. Lett.*, 23, 2,275-2,278, 1996.
- Heinson, G.S. and S.C. Constable, The electrical conductivity of the oceanic upper mantle, *Geophys. J. Int.*, 110, 159-179, 1992.
- Lilley, F. E. M., Magnetotelluric tensor decomposition: Part I, Theory for a basic procedure, *Geophysics*, 63, 1885-1897, 1998.
- Navin, D.A., C. Peirce and M.C. Sinha, RAMESSES II - Evidence for accumulated melt beneath a slow spreading ridge from wide-angle and multichannel reflection seismic profiles, *Geophys. J. Int.*, 135, 746-772, 1998.
- Mackie, R.L., T.R. Madden and P.E. Wannamaker, Three dimensional magnetotelluric modelling using difference equations: Theory and comparisons to integral equation solutions, *Geophysics*, 58, 215-226, 1993.
- MacGregor, L.M., M.C. Sinha and S.C. Constable, RAMESSES III - controlled source electromagnetic sounding of the Reykjanes Ridge at 57° 45' N, *Geophys. J. Int.*, 135, 773-789, 1998.
- Sinha, M.C., S.C. Constable, C. Peirce, C., A. White, G.S. Heinson, L.M. MacGregor and D.A. Navin, Magmatic processes at slow spreading ridges: implications of the RAMESSES experiments, Mid-Atlantic Ridge at 57° N, *Geophys. J. Int.*, 135, 731-745, 1998.
- Sinha, M.C., D.A. Navin, L.M. MacGregor, S.C. Constable, C. Peirce, A. White, G.S. Heinson and M.A. Inglis, Evidence for accumulated melt beneath the slow-spreading Mid-Atlantic Ridge, *Phil. Trans. R. Soc. Lond.*, 355, 233-253, 1997.
- Wannamaker, P.E., J.A. Stodt, and L. Rijo, A stable finite element solution for two-dimensional magnetotelluric modelling, *Geophys. J. R. astr. Soc.*, 88, 277-296, 1986.

G.S. Heinson

Department of Geology and Geophysics, University of Adelaide
Adelaide SA 5005, Australia (gheinson@geology.adelaide.edu.au)

S.C. Constable

Scripps Institution of Oceanography, UCSD, La Jolla CA 92093-0225, USA (sconstable@ucsd.edu)

A. White

School of Chemistry, Physics and Earth Sciences, Flinders
University of South Australia, Adelaide SA 5042, Australia
(awhite@cs.flinders.edu.au)

Received February 3, 2000 Revised April 25, 2000

Accepted May 11, 2000